Transient Analysis of Coupled, Tapered Transmission Lines with Arbitrary Nonlinear Terminations

Kyung S. Oh, *Student Member, IEEE,* and Jose E. Schutt-Aine *Member, IEEE*

Abstract—**In this paper, a fast and efficient method to simulate the time-domain transient response of coupled, tapered transmission lines is presented. A time-domain scattering parameter formulation is used to derive the simple closed-form expression for the voltage variables for uniform lossless lines; then, this expression is applied to tapered lines by dividing the lines into many uniform sections. Computational efficiency and stability are achieved using recursive time-domain algorithms. The method that assumes a quasi-TEM mode of propagation is applicable to nonlinear terminations and inhomogeneous dielectric media. Memory requirement is minimized and is independent of the number of time steps. Simulation results when compared with experimental simulations indicated a good level of agreement.**

I. Introduction

TAPERED microstrip transmission lines are often used as delay equalizers, impedance transformers, and impedance matching sections in microwave circuits. Currently, tapered lines are also appearing in digital integrated circuit applications as interconnections due to the recent development of the tape automated bonding (TAB) technology. A substantial amount of work has been devoted to the study of these structures [1]–[9], which have been investigated from the design viewpoint [8]. Syahkal and Davies [9] used the spectral domain technique to analyze tapered structures, while Protonotarios and Wing [8] characterized the line in term of its ABCD parameters to discuss the properties of the lines. Mehalic and Mittra [1] modeled tapered lines using an iteration-perturbation approach from which the frequency-dependent scattering parameters were extracted and used to simulate the time-domain voltage response. On the other hand, Rao *et al.* [10] developed a method to calculate the input impedance of a tapered line with arbitrary loads. In general, limited effort has been devoted to the study of transient and pulse degradations through coupled, tapered transmission lines [1]–[6].

The method presented in this paper is based on the time-domain scattering parameter approach. Although scattering parameters have been widely used in the frequency-domain (steady state) analysis of microwave circuit design, they are rarely used in the time-domain (transient) analysis; recently, they have been used for the time-domain simulation of uniform transmission lines with nonlinear terminations [11]. The advantages of scattering parameters over other network parameters such as the H-, Y-, or, Z-parameters become apparent when distributed networks are analyzed; in such situations, the scattering parameter approach will result in better numerical stability and simplicity. First, the method used in [11] is extended to formulate the transient response of coupled, tapered transmission lines. Scattering parameter transfer functions are used to derive recursion relations for the voltage solutions as a function of time. The algorithm thus implemented can be conveniently incorporated into a computer program for simulation.

Manuscript received October 7, 1991; revised June 17, 1992. This work was supported by the National Science Foundation under Grant ECS-89-13116 and by the Office of Naval Research under Grant N00014-90-J-1270.

The authors are with the Electromagnetic Communication Laboratory, Department of Electrical and Computer Engineering, University of Illinois, Urbana, IL 61801-2991.

IEEE Log Number 9204483.

II. Scattering Parameters of Coupled Uniform Lines

The frequency domain characteristics of coupled uniform lines, shown in Fig. 1(a), can be analyzed in terms of scattering parameters employing the notion of a two-port network, and using a scattering approach, the analysis of the system can be conveniently broken down into two parts: one which relates the voltage variables in the test lines while the other links these voltage variables with the termination conditions. Reference lines are first inserted at both ends of the test lines; Fig. 1(b) shows a single-line system with reference lines inserted. It should be pointed out that reference lines are nonphysical and, furthermore, with the flexibility in the choice of these reference lines, a scattering parameter approach will yield a more simplified solution. Now defining modal voltage coefficient vectors $\boldsymbol{A}_1, \boldsymbol{A}_2, \boldsymbol{B}_1$, and $\boldsymbol{B}_2$, at the transition planes, the scattering parameter matrices of a uniform N-line system, $\boldsymbol{S}_{11}, \boldsymbol{S}_{12}, \boldsymbol{S}_{21}$, and $\boldsymbol{S}_{22}$, satisfy the following relations in the reference lines:

$$\boldsymbol{B}_1 = \boldsymbol{S}_{11}\boldsymbol{A}_1 + \boldsymbol{S}_{12}\boldsymbol{A}_2 \tag{1a}$$

$$\boldsymbol{B}_2 = \boldsymbol{S}_{21}\boldsymbol{A}_1 + \boldsymbol{S}_{22}\boldsymbol{A}_2 \tag{1b}$$

where $\boldsymbol{A}_i$ and $\boldsymbol{B}_i$ are the incident and reflected modal voltage vectors, and the subscript 1 indicates the near ends, while the subscript 2 indicates the far ends assuming the source is located at the near ends, and the line voltage and current values can be recovered from

$$\boldsymbol{V}_i = \boldsymbol{E}_T^{-1}[\boldsymbol{A}_i + \boldsymbol{B}_i] \tag{2a}$$

$$\boldsymbol{I}_i = \boldsymbol{H}_T^{-1}\boldsymbol{Z}_T^{-1}[\boldsymbol{A}_i - \boldsymbol{B}_i] \quad i = 1, 2 \tag{2b}$$

where

$$\boldsymbol{E}_T\boldsymbol{L}_T\boldsymbol{C}_T\boldsymbol{E}_T^{-1} = \boldsymbol{H}_T\boldsymbol{C}_T\boldsymbol{L}_T\boldsymbol{H}_T^{-1} = \boldsymbol{\Lambda}_T^2 \tag{2c}$$

$$\boldsymbol{Z}_T = \boldsymbol{\Lambda}_T^{-1}\boldsymbol{E}_T\boldsymbol{L}_T\boldsymbol{H}_T^{-1} \tag{2d}$$

Here, the ith rows of $\boldsymbol{E_r}$ and $\boldsymbol{H_r}$ are the voltage and current eigenvectors corresponding to the ith mode, and $\boldsymbol{Z_r}$ is the modal impedance matrix while the subscript r denotes the reference line [11]. A time-domain formulation can be directly obtained by taking an inverse Fourier transform of (1):

$$\boldsymbol{b}_1(t) = \boldsymbol{s}_{11}(t) * \boldsymbol{a}_1(t) + \boldsymbol{s}_{12}(t) * \boldsymbol{a}_2(t) \tag{3a}$$

$$\boldsymbol{b}_2(t) = \boldsymbol{s}_{21}(t) * \boldsymbol{a}_1(t) + \boldsymbol{s}_{22}(t) * \boldsymbol{a}_2(t) \tag{3b}$$

Lower-case characters indicate the time domain, and each term is the inverse transform of the corresponding term in (1). The above equations relate incident wave vectors to reflected waves through convolution in the test lines, and the equations relating these wave vectors to termination conditions are given by

$$\boldsymbol{a}_1(t) = \boldsymbol{T}_1(t)\boldsymbol{g}_1(t) + \boldsymbol{\Gamma}_1(t)\boldsymbol{b}_1(t) \tag{4a}$$

$$\boldsymbol{a}_2(t) = \boldsymbol{T}_2(t)\boldsymbol{g}_2(t) + \boldsymbol{\Gamma}_2(t)\boldsymbol{b}_2(t) \tag{4b}$$

where $\boldsymbol{g_i}(t)$ is the modal source voltage vector, and $\boldsymbol{T_i}$ and $\boldsymbol{\Gamma_i}$ are the transmission and reflection coefficient matrices at the junction of the reference lines and the termination and are defined by

$$\boldsymbol{T_i}(t) = [\boldsymbol{I} + \boldsymbol{E_r}\boldsymbol{Z_i}(t)\boldsymbol{L_r^{-1}}\boldsymbol{E_r^{-1}}\boldsymbol{\Lambda_r}]^{-1} \tag{5a}$$

$$\boldsymbol{\Gamma_i}(t) = [\boldsymbol{I} + \boldsymbol{E_r}\boldsymbol{Z_i}(t)\boldsymbol{L_r^{-1}}\boldsymbol{E_r^{-1}}\boldsymbol{\Lambda_r}]^{-1} \cdot [\boldsymbol{I} - \boldsymbol{E_r}\boldsymbol{Z_i}(t)\boldsymbol{L_r^{-1}}\boldsymbol{E_r^{-1}}\boldsymbol{\Lambda_r}]; \quad i = 1, 2 \tag{5b}$$

where $\boldsymbol{Z_i}(t)$ and $\boldsymbol{I}$ are the impedance and identity matrices, respectively, and $\boldsymbol{\Lambda_r}$ is a diagonal eigenvalue matrix whose elements are given by $[\boldsymbol{\Lambda_r}]_{ii} = 1/\nu_{mi}$, where ν_{mi} is the velocity of propagation of the ith mode. It should be noticed that since the termination is lumped, the termination relations, (4) and (5), do not require convolutions and are only associated with the instantaneous values of the voltage and waves and terminations; thus it is applicable to nonlinear terminations. Moreover, when terminations are linear, the impedance matrices become time independent, and these equations have to be calculated only once. By matching the voltages at boundaries, frequency domain modal scattering parameters for lossless lines can be obtained:

$$\boldsymbol{S}_{11} = \boldsymbol{S}_{22} = \boldsymbol{T}^{-1}[\boldsymbol{\Gamma} - \boldsymbol{X}\boldsymbol{\Gamma}\boldsymbol{X}][\boldsymbol{I} - \boldsymbol{\Gamma}\boldsymbol{X}\boldsymbol{\Gamma}\boldsymbol{X}]^{-1}\boldsymbol{T} \tag{6a}$$

$$\boldsymbol{S}_{12} = \boldsymbol{S}_{21} = 2\boldsymbol{E_r}\boldsymbol{E}^{-1}[\boldsymbol{I} - \boldsymbol{\Gamma}]\boldsymbol{X}[\boldsymbol{I} - \boldsymbol{\Gamma} - \boldsymbol{X}\boldsymbol{\Gamma}\boldsymbol{X}]^{-1}\boldsymbol{T} \tag{6b}$$

where $\boldsymbol{X}$ is the diagonal matrix with $[\boldsymbol{X}]_{ii} = e^{-j\omega d/\nu_{mi}}$, and $\boldsymbol{\Gamma}$ and $\boldsymbol{T}$ are the reflection and transmission coefficient matrices at the junction of the reference lines and the test lines and are defined by

$$\boldsymbol{\Gamma} = [\boldsymbol{I} + \boldsymbol{E}\boldsymbol{E_r^{-1}}\boldsymbol{Z_r}\boldsymbol{H_r}\boldsymbol{H}^{-1}\boldsymbol{Z_m^{-1}}]^{-1} \cdot [\boldsymbol{I} - \boldsymbol{E}\boldsymbol{E_r^{-1}}\boldsymbol{Z_r}\boldsymbol{H_r}\boldsymbol{H}^{-1}\boldsymbol{Z_m^{-1}}] \tag{7a}$$

$$\boldsymbol{T} = [\boldsymbol{I} + \boldsymbol{E}\boldsymbol{E_r^{-1}}\boldsymbol{Z_r}\boldsymbol{H_r}\boldsymbol{H}^{-1}\boldsymbol{Z_m^{-1}}]^{-1}\boldsymbol{E}\boldsymbol{E_r^{-1}}. \tag{7b}$$

Again, the subscript r is used to distinguish between the variables for the reference lines and for the test lines. Now using the fact that the reference system consists of arbitrary nonphysical lines, the test line can be chosen to be equivalent to the reference lines. Then, we have

$$\boldsymbol{\Gamma} = 0 \tag{8a}$$

$$\boldsymbol{S}_{11} = \boldsymbol{S}_{22} = 0 \tag{8b}$$

$$\boldsymbol{S}_{12} = \boldsymbol{S}_{21} = \boldsymbol{X} \tag{8c}$$

With the above results, the convolution in (3) simplifies to

$$\boldsymbol{b}_1(t) = \boldsymbol{a}_2\left(t - \frac{d}{\nu_m}\right) \tag{9a}$$

$$\boldsymbol{b}_2(t) = \boldsymbol{a}_1\left(t - \frac{d}{\nu_m}\right) \tag{9b}$$

where the jth element of $\boldsymbol{a}_1(t - d/\nu_m)$ is the jth element of a_1 at $t - d/\nu_m$. Now $\boldsymbol{a}_i$ and $\boldsymbol{b}_i$ can be calculated using (4), (5), and (9), and the total line voltages and currents are recovered by using (2).

Fig. 1(c) illustrates the final results in terms of a signal flow graph representation of the time-domain scattering parameters of the lossless transmission line system. The nodes represent modal voltage waves and the branches designate the modal scattering parameters. Although the branches for $\boldsymbol{S}_{11}$ and $\boldsymbol{S}_{22}$ are not drawn due to the final results, they should be included in the general analysis. In the following section, this flow graph representation will be extensively used to analyze tapered lines.

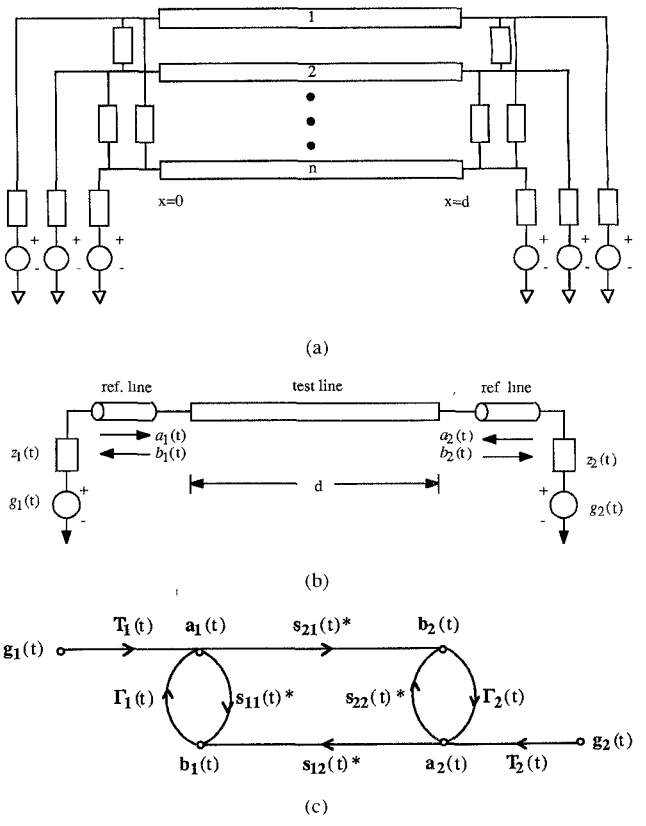

Fig. 1. (a) Topological representation of a uniform n-line system. (b) Single-line system with reference lines. (c) Time-domain flow-graph representation of (a). The * sign indicates a convolution in the time domain.

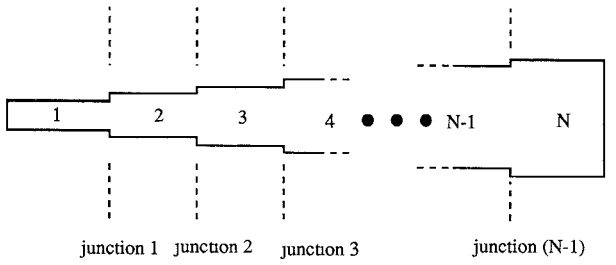

Fig. 2. Approximation of tapered line by cascading sections of uniform lines of different widths.

III. Formulation for Tapered Line System

In this section, the formulation of coupled, tapered lines is presented based on the results obtained from the previous section. A tapered line system is first approximated by cascading a large number of uniform coupled line sections as shown in Fig. 2. In this analysis, the fringing field due to junction discontinuity of these line sections is neglected by assuming that a sufficiently large number of sections is used, which can be further justified by recalling the nature of the original tapering geometry in which there is no abrupt junction discontinuity. In general, each section of uniform coupled lines can be analyzed by inserting a reference system at both ends of the section. The reference system consists of an array of ideal uniform transmission lines. Since the reference system is arbitrary, it is convenient to make it equivalent to the test system that leads to simpler expressions. Consequently, each section of the tapered line system will be described in terms of a different reference system. Connecting the flow graphs associated with adjacent sections of the jth junction will then introduce the branch parameters $\boldsymbol{T_j}, \boldsymbol{\Gamma_j}, \boldsymbol{T'_j}$, and $\boldsymbol{\Gamma'_j}$ which account for the change in the reference system from the jth to the $(j+1)$th section as shown in Fig. 3(a), (b), and (c) for the jth junction and the first and last junctions, respectively.

Solution for the Voltage Waves at an Arbitrary Junction

Based on the study of the flow graph in Fig. 3(a), we can now write the equations relating the modal voltage wave vectors of the middle sections of the tapered line segments as follows:

$$\boldsymbol{u_j}(t) = \boldsymbol{T_j}\boldsymbol{w'_{j-1}}(t) + \boldsymbol{\Gamma'_j}\boldsymbol{w_j}(t) \tag{10a}$$

$$\boldsymbol{w_j}(t) = \boldsymbol{S}_{12(j)}(t) * \boldsymbol{u'_j}(t) = \boldsymbol{u'_j}\left(t - \frac{d}{v_j}\right) \tag{10b}$$

$$\boldsymbol{u'_j}(t) = \boldsymbol{T'_{j+1}}\boldsymbol{w_{j+1}}(t) + \boldsymbol{\Gamma_{j+1}}\boldsymbol{w'_j}(t) \tag{10c}$$

$$\boldsymbol{w'_{j-1}}(t) = \boldsymbol{S}_{21(j-1)}(t) * \boldsymbol{u_{j-1}}(t) = \boldsymbol{u_{j-1}}\left(t - \frac{d}{v_{j-1}}\right) \tag{10d}$$

where $\boldsymbol{u_j}, \boldsymbol{w_j}, \boldsymbol{u'_j}$, and, $\boldsymbol{w'_j}$ are the incident and reflected modal voltage wave vectors of the source and load sides of the jth section, respectively, and the lengths of each sections are assumed to be the same for simplicity of notation. $\boldsymbol{T_j}, \boldsymbol{\Gamma_j}, \boldsymbol{T'_j}$, and $\boldsymbol{\Gamma_j}$ are the modal transmission and reflection coefficient matrices associated with the $(j-1)$th junction which is located between the $(j-1)$th and jth sections. Then, by satisfying the boundary condition at the $(j-1)$th junction, the expressions of $\boldsymbol{T_j}, \boldsymbol{\Gamma_j}, \boldsymbol{T'_j}$, and $\boldsymbol{\Gamma_j}$ at the junction can be obtained:

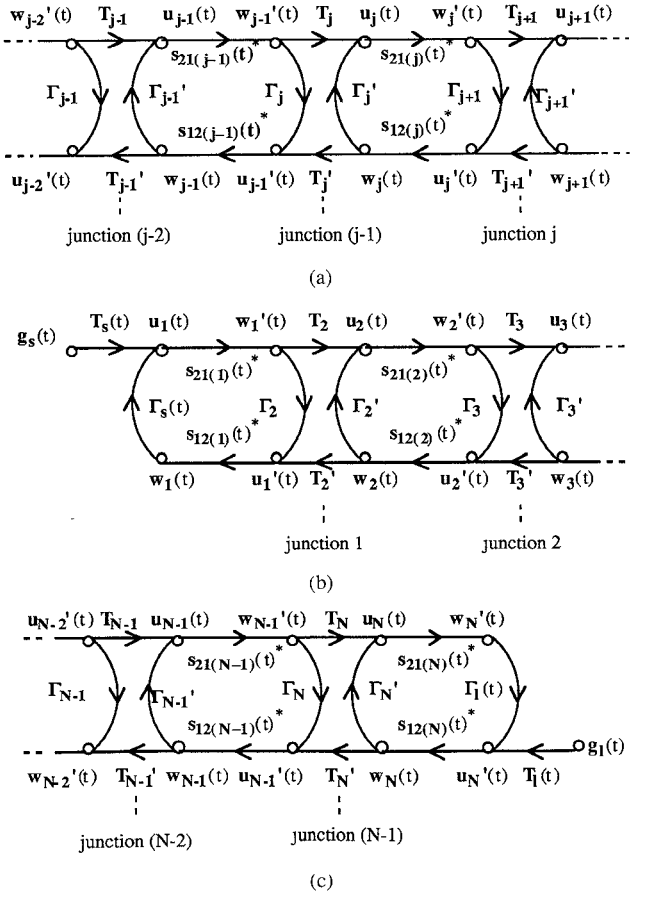

Fig. 3. Time-domain flow graphs for (a) middle sections, (b) source end, and (c) load end of coupled, tapered lines. The * sign indicates a convolution in the time domain.

$$\boldsymbol{T_j} = 2[\boldsymbol{I} + \boldsymbol{E_j}\boldsymbol{E_{j-1}^{-1}}\boldsymbol{Z_{j-1}}\boldsymbol{H_{j-1}}\boldsymbol{H_j^{-1}}\boldsymbol{Z_j^{-1}}]^{-1}\boldsymbol{E_j}\boldsymbol{E_{j-1}^{-1}} \tag{11a}$$

$$\boldsymbol{T'_j} = 2[\boldsymbol{I} + \boldsymbol{E_{j-1}}\boldsymbol{E_j^{-1}}\boldsymbol{Z_j}\boldsymbol{H_j}\boldsymbol{H_{j-1}^{-1}}\boldsymbol{Z_{j-1}^{-1}}]^{-1}\boldsymbol{E_{j-1}}\boldsymbol{E_j^{-1}} \tag{11b}$$

$$\boldsymbol{\Gamma_j} = [\boldsymbol{I} + \boldsymbol{Z_{j-1}}\boldsymbol{H_{j-1}}\boldsymbol{Z_j^{-1}}\boldsymbol{E_j}\boldsymbol{E_{j-1}^{-1}}]^{-1} \cdot [\boldsymbol{I} - \boldsymbol{Z_{j-1}}\boldsymbol{H_{j-1}}\boldsymbol{H_j^{-1}}\boldsymbol{Z_j^{-1}}\boldsymbol{E_j}\boldsymbol{E_{j-1}^{-1}}] \tag{11c}$$

$$\boldsymbol{\Gamma'_j} = [\boldsymbol{I} + \boldsymbol{Z_j}\boldsymbol{H_j}\boldsymbol{H_{j-1}^{-1}}\boldsymbol{Z_{j-1}^{-1}}\boldsymbol{E_{j-1}}\boldsymbol{E_j^{-1}}]^{-1} \cdot [\boldsymbol{I} - \boldsymbol{Z_j}\boldsymbol{H_j}\boldsymbol{H_{j-1}^{-1}}\boldsymbol{Z_{j-1}^{-1}}\boldsymbol{E_{j-1}}\boldsymbol{E_j^{-1}}] \tag{11d}$$

where the subscript j denotes the jth section; a detailed derivation is given in the Appendix. Substituting (10c) and (10d) into (10a) and (10b), (10) can be further simplified as follows:

$$\boldsymbol{u_j}(t) = \boldsymbol{T_j}\boldsymbol{u_{j-1}}\left(t - \frac{d}{v_{j-1}}\right) + \boldsymbol{\Gamma'_j}\boldsymbol{w_j}(t) \tag{12a}$$

$$\boldsymbol{w_j}(t) = \boldsymbol{T'_{j+1}}\boldsymbol{w_{j+1}}\left(t - \frac{d}{v_j}\right) + \boldsymbol{\Gamma_{j+1}}\boldsymbol{u_j}\left(t - \frac{2d}{v_j}\right) \tag{12b}$$

From the above equations, it is clear that the forward and backward voltage waves of the jth junction can be obtained from the history of the adjacent junctions ($(j-1)$th and $(j+1)$th), and from the voltage continuity relation, the total voltage at any side of the junction can always be obtained.

Solution for Voltages at the Source and Load Ends

Equations for the voltage vectors at the two ends of the tapered line system can be easily derived following the above arguments and using the flow graph in Fig. 3(b) and (c). For the source end, the expressions are given by

$$\boldsymbol{u}_1(t) = \boldsymbol{T_s}(t)\boldsymbol{g_s}(t) + \boldsymbol{\Gamma_s}(t)\boldsymbol{w}_1(t) \tag{13a}$$

$$\boldsymbol{w}_1(t) = \boldsymbol{T}'_2\boldsymbol{w}_2\left(t - \frac{d}{v_1}\right) + \boldsymbol{\Gamma}_2\boldsymbol{u}_1\left(t - \frac{2d}{v_1}\right) \tag{13b}$$

To obtain the total line voltage at the load end, the values of $\boldsymbol{u'_N}$ and $\boldsymbol{w'_N}$ are required instead of $\boldsymbol{u_N}$ and $\boldsymbol{w_N}$; therefore, including the expressions for $\boldsymbol{u'_N}$ and $\boldsymbol{w'_N}$, we have

$$\boldsymbol{u'_N}(t) = \boldsymbol{T_l}(t)\boldsymbol{g_l}(t) + \boldsymbol{\Gamma_l}(t)\boldsymbol{w'_N}(t) \tag{14a}$$

$$\boldsymbol{w'_N}(t) = \boldsymbol{u_N}\left(t - \frac{d}{v_N}\right) \tag{14b}$$

$$\boldsymbol{u_N}(t) = \boldsymbol{T_N}\boldsymbol{u_{N-1}}\left(t - \frac{d}{v_{N-1}}\right) + \boldsymbol{\Gamma'_N}\boldsymbol{w_N}(t) \tag{14c}$$

$$\boldsymbol{w_N}(t) = \boldsymbol{u'_N}\left(t - \frac{d}{v_N}\right). \tag{14d}$$

Here, $\boldsymbol{gt}$ is the modal voltage source, and the subscripts s and l represent the source and load sides of the ith segment, respectively. The reflection and transmission coefficient matrices at two ends, $\boldsymbol{T_s}(t), \boldsymbol{\Gamma_s}(t), \boldsymbol{T_l}(t)$, and $\boldsymbol{\Gamma_l}(t)$, can be calculated using (5) in Section II by replacing the subscripts 1 and 2 with s and l, accordingly. Equations (12), (13), and (14) can thus be used to simulate the overall system at each time step; in particular, the line voltage vectors at the two ends are recovered using

$$\boldsymbol{v_s}(t) = \boldsymbol{E}_1^{-1}[\boldsymbol{u}_1(t) + \boldsymbol{w}_1(t)] \tag{15a}$$

$$\boldsymbol{i_s}(t) = \boldsymbol{H}_1^{-1}\boldsymbol{Z}_1^{-1}[\boldsymbol{u}_1(t) - \boldsymbol{w}_1(t)] \tag{15b}$$

$$\boldsymbol{v_l}(t) = \boldsymbol{E_N}^{-1}[\boldsymbol{u'_N}(t) + \boldsymbol{w'_N}(t)] \tag{15c}$$

$$\boldsymbol{i_l}(t) = \boldsymbol{H_N}^{-1}\boldsymbol{Z_N}^{-1}[\boldsymbol{u'_N}(t) - \boldsymbol{w'_N}(t)] \tag{15d}$$

Considering the computer memory space requirement of the above results, the number of voltage variables to be calculated for N sections of lines is $(2N+2)$: two voltage variables $\boldsymbol{u_j}$ and $\boldsymbol{w_j}$, for each section (Equations (12), (13), (14c), and (14d)), and two additional voltage variables, $\boldsymbol{u'_j}$ and $\boldsymbol{w'_j}$, for load end (Equations (14a) and (14b)). Furthermore, since (12), (13), and (14) relate values of these voltage variables at the current time step to the values calculated at $(t - 2d/\nu_j)$ and $(t - d/\nu_j)$, these voltage variables have to be stored at most for $2d/\nu_j$, which is twice the time required for the ith mode voltage wave to travel from one side of the section to the other side. Thus, the memory location required from the above results is linearly proportional to the number of sections used to approximate the tapered lines and the size of the time step, and is independent of the number of time steps or the length of the simulation period.

IV. Simulation Results

A computer simulation program was implemented based on the previous results, and was tested for single- and three-line cases. The space variations of the test structures were all linear, and specific geometries and dimensions are shown in Fig. 4. First, for the single-line case, the dielectric thickness was 59 mils, and the relative dielectric constant was 2.55. The input pulse used to simulate the single line had rise and fall times of 1 ns and a pulse width of 10 ns with a maximum voltage of 4 V. The static formulas had been used to obtain the effective permittivity and line impedance for each uniform line section [12]. Fig. 5 shows the simulated results of voltage waveforms at both ends of the line with excitation of the input pulse at the narrow and wide ends. For all simulated cases, the line was open ended with a source impedance of 50 Ω. Tapering effects are shown with slowly decaying and rising edges between the sharp transition edges. For the three-line case, the dielectric thickness was 31 mils and the relative dielectric constant was 4.7. Rise and fall times of 1.6 ns and pulse width of 17 ns with a maximum voltage of 1.58 V are used for the input pulse. Circuit parameters of the lines were extracted using the spectral-iterative technique in conjunction with the minimization in the boundary condition error. Experiments are also given to verify the results. The middle line was used to drive the signal with the same source impedance as in the previous case. All lines were open ended at both sides except for the source end of the driving line and load end of the sense line, which is one of the outer lines. The short and open-ended terminations are used at the load end of the sense line which is located at the opposite side of the source end of the driving line. Fig. 6 shows the comparison of the computer simulation with the corresponding experimental results. Good agreement was found except for any parasitic side effects.

V. Conclusions

A new technique to simulate the transient response of coupled, tapered lines is introduced based on time-domain scattering parameters. In contrast with other known methods, the present method avoids the use of convolution or the spectral domain approach and thus achieved high computational efficiency and accuracy. The linear time dependency and constant memory space requirement were achieved with respect to simulation time. A computer program was written based on the final results, and simulation results from this program showed good agreement with the experimental results and other existing techniques. Although the present method applied only to tapered lines, it can be further generalized to analyze any nonuniform transmission lines or lines with distributed loadings. Currently, the authors are also studying the improved version of this method with constant or frequency-dependent loss.

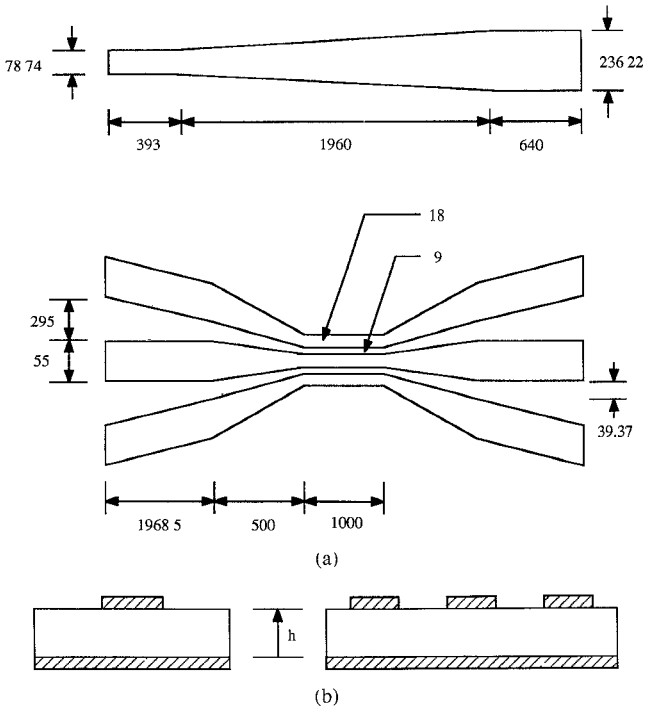

Fig. 4. (a) Planar and (b) cross-sectional views of the simulated tapered microstrip lines. Units are in mils.

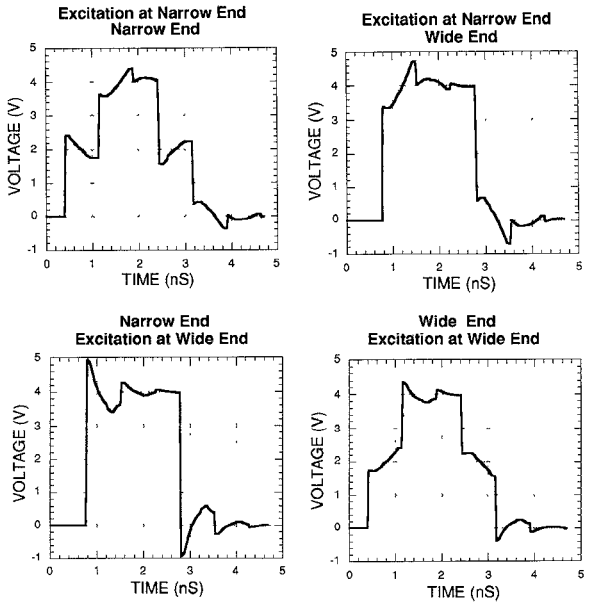

Fig. 5. Computer simulation plots for the single line in Fig. 4(a) The input pulse characteristics are $V_{\max} = 4$ V, $t_d = 0.4$ ns, $t_w = 2$ ns, and $t_r = t_f = 25$ ps.

APPENDIX

Derivation of the Reflection and Transmission Coefficient Matrices at the Junction

Let us consider the junction of two segments of coupled, tapered lines, Segments 1 and 2, and denote the incident modal voltage wave that arrives at the junction from Segment 1 by $\boldsymbol{A}$, and the reflected and transmitted modal voltages by $\boldsymbol{B}$ and $\boldsymbol{C}$, respectively. Then, the total line voltages and currents at

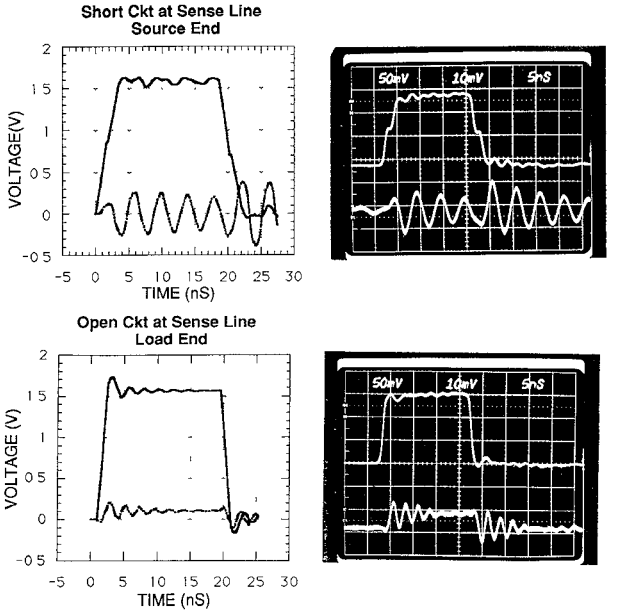

Fig. 6. Computer simulation results for the three-line case in Fig. 4(b). The voltages at driving and sense lines are represented by the solid and dotted lines, respectively.

Segments 1 and 2, denoted by $\boldsymbol{V}_1, \boldsymbol{V}_2, \boldsymbol{I}_1$, and $\boldsymbol{I}_2$, are given by the following expressions:

$$\boldsymbol{V}_1 = \boldsymbol{E}_1^{-1}[\boldsymbol{A} + \boldsymbol{B}] \tag{A1a}$$

$$\boldsymbol{V}_2 = \boldsymbol{E}_2^{-1}\boldsymbol{C} \tag{A1b}$$

$$\boldsymbol{I}_1 = \boldsymbol{H}_1^{-1}\boldsymbol{Z}_{\boldsymbol{m}1}^{-1}[\boldsymbol{A} - \boldsymbol{B}] \tag{A2a}$$

$$\boldsymbol{I}_2 = \boldsymbol{H}_2^{-1}\boldsymbol{Z}_{\boldsymbol{m}2}^{-1}\boldsymbol{C} \tag{A2b}$$

Since these total line voltages and currents at the junction must be equal, we have

$$\boldsymbol{E}_1^{-1}[\boldsymbol{A} + \boldsymbol{B}] = \boldsymbol{E}_2^{-1}\boldsymbol{C} \tag{A3a}$$

$$\boldsymbol{H}_1^{-1}\boldsymbol{Z}_{\boldsymbol{m}1}^{-1}[\boldsymbol{A} - \boldsymbol{B}] = \boldsymbol{H}_2^{-1}\boldsymbol{Z}_{\boldsymbol{m}2}^{-1}\boldsymbol{C}. \tag{A3b}$$

Now solving the above equations for $\boldsymbol{B}$ and $\boldsymbol{C}$ in terms of $\boldsymbol{A}$, we obtain

$$\boldsymbol{B} = [\boldsymbol{I} + \boldsymbol{P}]^{-1}[\boldsymbol{I} - \boldsymbol{P}]\boldsymbol{A} \tag{A4a}$$

$$\boldsymbol{C} = 2[\boldsymbol{I} + \boldsymbol{Q}]^{-1}\boldsymbol{E}_2\boldsymbol{E}_1^{-1}\boldsymbol{A} \tag{A4b}$$

where

$$\boldsymbol{P} = \boldsymbol{Z}_1\boldsymbol{H}_1\boldsymbol{H}_2^{-1}\boldsymbol{Z}_2^{-1}\boldsymbol{E}_2\boldsymbol{E}_1^{-1} \tag{A4c}$$

$$\boldsymbol{Q} = \boldsymbol{E}_2\boldsymbol{E}_1^{-1}\boldsymbol{Z}_1\boldsymbol{H}_1\boldsymbol{H}_2^{-1}\boldsymbol{Z}_2^{-1} \tag{A4d}$$

Finally, the expressions for $\boldsymbol{\Gamma}$ and $\boldsymbol{T}$ are then given by

$$\boldsymbol{\Gamma} = [\boldsymbol{I} + \boldsymbol{Z}_1\boldsymbol{H}_1\boldsymbol{H}_2^{-1}\boldsymbol{Z}_2^{-1}\boldsymbol{E}_2\boldsymbol{E}_1^{-1}]^{-1} \cdot [\boldsymbol{I} - \boldsymbol{Z}_1\boldsymbol{H}_1\boldsymbol{H}_2^{-1}\boldsymbol{Z}_2^{-1}\boldsymbol{E}_2\boldsymbol{E}_1^{-1}] \tag{A5a}$$

$$\boldsymbol{T} = 2[\boldsymbol{I} + \boldsymbol{E}_2\boldsymbol{E}_1^{-1}\boldsymbol{Z}_1\boldsymbol{H}_1\boldsymbol{H}_2^{-1}\boldsymbol{Z}_2^{-1}]^{-1}\boldsymbol{E}_2\boldsymbol{E}_1^{-1} \tag{A5b}$$

Similarly, expressions for $\boldsymbol{\Gamma}'$ and $\boldsymbol{T}'$ can be obtained simply by interchanging the subscripts 1 and 2 from the above equations.

REFERENCES

[1] M. A. Mehalic and R. Mittra, "Investigation of tapered multiple microstrip lines for VSLI circuits," *IEEE Trans. Microwave Theory Tech.*, vol. 38, pp. 1559–1567, Nov. 1990.

[2] . A. Palusinski and A. Lee, "Analysis of transients in nonuniform and uniform multiconductor transmission lines," *IEEE Trans. Microwave Theory Tech.*, vol. 37, pp. 127–138, Jan. 1989.

[3] C. Hsue and C. C. Hechtman, "Transient analysis of nonuniform, high-pass transmission lines," *IEEE Trans. Microwave Theory Tech.*, vol. 38, pp. 1023–1030, Aug. 1990.

[4] J. L. Hill and D. Mathews, "Transient analysis of systems with exponential transmission lines," *IEEE Trans. Microwave Theory Tech.*, vol. 25, pp. 777–783, Sept. 1977.

[5] Y.-C. E. Yang, J. A. Kong, and Q. Gu, "Time-domain perturbation analysis of nonuniformly coupled transmission lines," *IEEE Trans. Microwave Theory Tech.*, vol. 33, pp. 1120–1130, Nov. 1985.

[6] A. S. AlFuhaid, "s-domain analysis of electromagnetic transients on nonuniform lines," *IEEE Trans. Power Delivery*, vol. 5, pp. 2072–2083, Nov. 1990.

[7] R. E. Collin, *Foundations for Microwave Engineering*. New York: McGraw Hill, 1966.

[8] E. N. Protonotarios and O. Wing, "Analysis and intrinsic properties of the general nonuniform transmission line," *IEEE Trans. Microwave Theory Tech.*, vol. 15, pp. 142–150, Mar. 1967.

[9] D. Mirshekar-Syahkal and J. B. Davies, "Accurate analysis of tapered planar transmission lines for microwave integrated circuits," *IEEE Trans. Microwave Theory Tech.*, vol. 29, pp. 123–128, Feb. 1981.

[10] K. N. Suryanarayana Rao, V. Mahadevan, and S. P. Kosta, "Analysis of straight tapered microstrip transmission lines-ASTMIC," *IEEE Trans. Microwave Theory Tech.*, vol. 25, p. 164, Feb. 1977.

[11] J. E. Schutt-Aine and R. Mittra, "Nonlinear transient analysis of coupled transmission lines," *IEEE Trans. Microwave Theory Tech.*, vol. CAS-36, pp. 959–967, July 1989.

[12] R. Owens, "Predicted frequency dependence of microstrip characteristic impedance using the planar-wave guide model," *Electron. Lett.*, vol. 12, pp. 269–270, May 1976.

Kyung S. Oh (S'91) was born in Pusan, S. Korea in 1965. He received the B.S. and M.S. degrees in electrical engineering from the University of Illinois at Urbana-Champaign in 1990 and 1992, respectively.

He is presently studying in the Graduate School of Electrical Engineering at the University of Illinois, where he has been engaged in research on modeling and simulation of high speed digital circuits.

Jose E. Schutt-Aine (M'82) received the B.S. degree from MIT in 1981, and his M.S. and Ph.D. degrees from the University of Illinois in 1984 and 1988, respectively.

Following his graduation from MIT he spent two years with Hewlett-Packard Microwave Technology Center in Santa Rosa, CA, where he worked as a device application engineer. While pursuing his graduate studies at the University of Illinois, he held summer positions at GTE Network Systems in Northlake, IL. He is presently serving on the faculty of the Department of Electrical and Computer Engineering at the University of Illinois as an Assistant Professor. Dr. Schutt-Aine's interests include microwave theory and measurements, electromagnetics, high-speed digital circuits, solid-state electronics, circuit design and electronic packaging.